Use of imaging spectroscopy to discriminate symptoms caused by *Heterodera schachtii* and *Rhizoctonia solani* on sugar beet

Christian Hillnhütter · Anne-Kathrin Mahlein · Richard Alexander Sikora · Erich-Christian Oerke

Abstract Diseases caused by nematodes and non-sporulating soil-borne fungi have low mobility and are likely to be suitable targets for precision agriculture applications. Sensors which assess the reflectance of plant leaves may be useful tools to detect soil-borne pathogens. The development of symptoms caused by the plant parasitic nematode *Heterodera schachtii* and the fungal pathogen *Rhizoctonia solani* anastomosis group 2-2IIIB alone or in combination was studied by leaf reflectance recorded with a hyperspectral imaging system (range 400–1000 nm) for 9 weeks twice per week. Three image processing methods were tested for their suitability to generate the most sensitive spectral information for disease detection. Nine spectral vegetation indices were calculated from spectra to correlate them to leaf symptom recordings. Supervised classification by spectral angle mapper was tested for the discrimination of leaf symptoms caused by the diseases. The symptoms of *Rhizoctonia* crown and root rot caused by *R. solani* and symptoms caused by *H. schachtii* induced modifications that could be detected by hyperspectral image analysis. *Rhizoctonia* crown and root rot symptom development in mixed inoculations was faster and more severe than in single inoculations, indicating complex interactions among fungus, nematode and plant. The results from this study under controlled conditions are currently used to transfer the sensor technology to the field.

Keywords Image processing · Spectral vegetation indices · Spectral angle mapper · Disease detection · Interrelationships · Soil-borne pathogens · Precision crop protection

C. Hillnhütter (✉) · A.-K. Mahlein · R. A. Sikora · E.-C. Oerke
Institute of Crop Science and Resource Conservation (INRES)—Phytomedicine,
Rheinische Friedrich-Wilhelms-Universität Bonn, Nussallee 9, 53115 Bonn, Germany
e-mail: chillnhu@uni-bonn.de; christian.hillnhuetter@gmx.de

Introduction

The plant parasitic nematode *Heterodera schachtii* (Schmidt) and the soil-borne fungal pathogen *Rhizoctonia solani* (Kühn) [teleomorph *Thanatephorus cucumeris* (Frank) Donk] are two major constraints in sugar beet production worldwide (Kiewnick et al. 2001; Schlang 1991). Above-ground symptoms caused by the root-colonizing beet cyst nematode (BCN) are stunted growth, decreased chlorophyll content and wilting of the canopy in the late cropping season due to water stress (Cooke 1987; Schmitz et al. 2006). *Rhizoctonia* crown and root rot (RCRR) caused by *R. solani* anastomosis group (AG) 2-2IIIB results in yellowing of leaves, which later become necrotic. Furthermore, symptoms include wilting, collapse and formation of a rosette of dying leaves on the soil (Herr 1996). Both soil-borne organisms occur in patches in the field, have low active mobility and induce above-ground symptoms on the canopy, which makes them suitable targets for precision agriculture tools. Disease detection by reflectance measurements of plant canopies and mapping of disease occurrence may help in the generation of management zones for disease control (Hillnhütter and Mahlein 2008). Disease control can include the site-specific application of nematicides or fungicides, if registered. Furthermore, site-specific sowing of sugar beet cultivars with different levels of tolerance or resistance against BCN and RCRR can be realized. Detection of RCRR early in the cropping season can be used for harvest of infested beets prior to severe harvest losses (Hillnhütter et al. 2011a).

Several studies have been conducted successfully on the detection of stresses caused by nematodes and soil-borne fungal pathogens on plant canopy reflectance by non-imaging multi- and hyperspectral sensors (Heath et al. 2000; Laudien 2005; Nutter et al. 2002). The potential of a non-imaging hyperspectral sensor and the calculation of spectral vegetation indices (SVIs), e.g., the normalized difference vegetation index (NDVI) for the assessment of symptoms caused by BCN and RCRR on sugar beet plants under controlled conditions was demonstrated by Hillnhütter et al. (2011b). In the present study, an imaging hyperspectral sensor was tested for the detection of above-ground symptoms of BCN and RCRR.

Imaging spectroscopy has several advantages over non-imaging spectro-radiometers (Kumar et al. 2001). Spatial resolution of non-imaging sensors is low and contains mixed information of plant material—diseased and non-diseased—and soil, whereas the information can be separated using imaging systems (Bravo 2006). Imaging spectroscopy is the fusion of imaging technology and spectroscopy, in which each pixel of the image is a vector of high-resolution spectral information (Noble et al. 2003). Until recently, this technology has been primarily used in remote sensing applications, but it has become available also for near-range hyperspectral imagery and has been identified as a tool with high potential for disease detection in crop production (Moshou et al. 2006).

For the detection of leaf pathogens by reflectance, it is important to eliminate the influence of soil reflectance on spectral information in order to obtain more sensitive data. Threshold levels of NDVI are often used to discriminate leaf reflectance from soil reflectance (Moshou et al. 2006). The NDVI was shown to be a suitable parameter for the discrimination of vegetation from background (Rouse et al. 1974). For the assessment of damage caused by soil-borne pathogens like *H. schachtii* and *R. solani*, however, soil reflectance may be used for the quantification of disease incidence and plant biomass which decreases with disease severity while the proportion of the soil increases.

Spectral vegetation indices are used routinely in remote sensing for the extraction of information from hyperspectral data. Correlations of SVIs with yield, nutrient supply or damage by pathogens have been reported for greenhouse and field experiments (Bajwa et al. 2010; Mahlein et al. 2010; Yang and Everitt 2002). As pigment content provides

information on the physiological state of leaves, pigment-specific SVIs may be correlated to symptoms caused by BCN or RCRR. By calculating ratios from several bands at different ranges of the spectrum, SVIs result in a reduction of data dimension and may provide information on the content of pigments or water, and also on the tissue structure of leaves (Mahlein et al. 2010).

Hyperspectral data may be also analysed using the spectral angle mapper (SAM) developed by Kruse et al. (1993), a supervised classification method. The SAM assesses the similarity of spectra of interest with n bands to reference spectra by calculating the n-dimensional angle between spectra. It has been successfully applied for the classification of different states of sorghum leaves (Yang et al. 2008) and in a variety of hyperspectral remote and near-range sensing applications (Clark et al. 2005; Feilhauer et al. 2010; Mundt et al. 2005; Qin et al. 2009). In this study, the method was tested for its suitability to differentiate healthy leaves from leaves with symptoms of yellowing, wilting or necrotic tissue.

The overall objective of this study was to examine the potential of near-range hyperspectral imaging to detect and identify sugar beet diseases caused by either BCN or RCRR alone, or both organisms in combination. More specific objectives were: (i) to test various methods of image pre-processing to obtain the most relevant spectral data for detection and discrimination of disease symptoms; (ii) to investigate the influence of soil reflectance on the correlation between SVIs and disease ratings; (iii) to test a supervised classification technique for identification of symptoms caused by BCN and RCRR.

Materials and methods

Organisms

Seeds of sugar beet, cultivar Alyssa (susceptible to *H. schachtii* and *R. solani*, KWS GmbH, Einbeck, Germany) were sown in multi-pots ($0.05 \times 0.5 \times 0.28$ m) and grown for 28 days at 25/22°C (day/night), $70 \pm 10\%$ relative humidity and a photo-period of 12 h d^{-1} (>300 µmol m^{-2} s^{-1}, Phillips SGR 140, Hamburg, Germany). After 4 weeks, plants were transplanted into boxes ($1.2 \times 0.8 \times 0.25$ m) containing 240 l substrate with sand, soil from C- and A-horizon, respectively, and Seramis® (Mars GmbH, Mogendorf, Germany) at a ratio of 2:0.6:0.4:0.4 (v/v). Thirty-two plants were planted into each box with 0.15 m spacing between plants within rows and a row width of 0.2 m. Each box comprised four rows with eight plants each. Plants were fertilized with 400 g long-term fertilizer Osmocote® Plus (15:9:12, Scotts, Maysville, OH, USA) per box.

Heterodera schachtii was from the institutes' stock cultures and was multiplied on *Brassica napus*, cultivar Akela (Feldsaaten Freudenberger, Krefeld, Germany), grown in sand. Cysts were extracted using a standard wet-screen decantation method and were transferred to Oostenbrink dishes filled with 5 mM ZnCl$_2$-solution for seven days to stimulate hatching of juveniles of larval stage 2 (J2) (Oostenbrink 1960). The J2 were washed on 25 µm sieves (Retsch, Haan, Germany), counted and subsequently used for inoculation of the plants.

Rhizoctonia solani (AG 2-2 IIIB) was provided by the Plant Protection Service of North Rhine-Westphalia. A sand-flour protocol developed by Zens et al. (2002) was used for inoculum production; 50 g of sand mixed with 1.5 g wheat flour and 7 ml tap water in a 200 ml Erlenmeyer flask sealed with a cotton plug was autoclaved at 121°C for 50 min. After cooling, the medium was inoculated with three mycelia pieces (Ø 5 mm) of *R. solani*

taken from cultures grown on potato dextrose agar (PDA) (24 g l^{-1} potato dextrose broth (PDB) [Becton, Dickinson and Company, Le Pont de Claix, France] + 18 g l^{-1} agar [AppliChem, Darmstadt, Germany]) for 14 days. The flasks were incubated at 24°C in the dark for 14 days and were shaken every second day to optimize fungal growth.

Inoculation

Rhizoctonia solani sand-flour inoculum (2.5 g) was placed into 5 cm deep cavities in the soil of the boxes before transferring the sugar beet seedlings onto the inoculum into the cavities which were finally filled up with substrate. Nematodes were inoculated into two cavities (3 cm deep) in the soil with a pipette tip near the base of the plant. Each cavity received 1 ml tap water with 3000 J2 of *H. schachtii* (=6000 J2 plant^{-1}).

The experiment included four treatments; untreated control plants; sugar beet inoculated with *H. schachtii* alone; inoculated with *R. solani* alone; inoculated with both organisms in combination. Each treatment had 32 plants and the experiment was conducted twice, which resulted in a total of 256 plants.

Evaluation of plants and pathogens

The experiments were terminated 9 weeks after inoculation. Fresh weight of beets and shoots were determined for each plant. The percentage surface rot of beets caused by *R. solani* was rated on a scale of: 0 = healthy, no symptoms, to 6 = beet completely rotted, plant dead (Zens et al. 2002). Leaf symptoms induced by RCRR were rated according to a protocol of Zens et al. (2002) which classifies wilting, yellowing or necrosis of leaves on a scale from 0 = plant healthy, no symptoms on petioles, to 6 = leaf brown and necrotic.

The number of eggs and juveniles of *H. schachtii* were determined after harvest by sampling 100 g of soil with a soil core sampling tool (Oakfield Apparatus Inc., Oakfield, WI, USA) from the sites where sugar beet plants had grown. The cysts of nematodes were extracted using a wet-screen decantation technique with a sieve combination of 500 and 250 μm aperture (Ayoub 1980). The cysts were transferred to 15 ml homogenization tubes (Braun, Melsungen, Germany) in which they were crushed. The number of eggs and J2 per plant was then counted under a stereoscope with 40-fold magnification in a 2 ml RAS-counting slide (Hooper et al. 2005) with sloping sides consisting of a 2 mm high plastic ring glued on a plastic plate of 75 × 37 mm.

Hyperspectral imaging

Data acquisition and pre-processing

Leaf reflectance of plants was recorded starting 5 days after inoculation (dai) to 64 dai twice per week. Hyperspectral images were obtained by a line scanner (ImSpector V10E, Spectral Imaging Ltd., Oulu, Finland) in combination with a mirror scanner, which was mounted under a rack specially constructed for this sensor. Images were recorded in a dark room and the sensor was surrounded by six ASD Pro-Lamps (Analytical Spectral Devices Inc., Boulder, CO, USA) in order to provide optimum illumination. The ImSpector has a spectral range from 400 to 1000 nm, a spectral resolution of 2.8 nm and a slit width of 14 mm. After focussing the camera using a black and white test target, the white reference (Spectral Imaging Ltd., Oulu, Finland) and the boxes with plants to be recorded were

placed in exactly the same position to the camera for each measurement. Images were obtained from 1.5 m above canopy with a spatial resolution of 0.2 cm^2 pixel^{-1}. The operator software SpectralCube (Spectral Imaging Ltd., Oulu, Finland) was used to record the images to the hard disc. First, the frame rate and the exposure time had to be optimized. A dark current image was taken by closing the shutter of the camera. Subsequently, the plants were recorded with the white reference and another image, with changed exposure time, without white reference.

The three images—dark current, white reference and raw image—obtained for each treatment were normalized using the program ENVI 4.6 + IDL 7.0 (ITT Visual Information Solutions, Boulder, CO, USA) by a special IDL tool. A normalized image was produced by comparing the raw image to the dark current image (minimum) and the white reference (maximum). The Savitzky–Golay smoothing filter (Savitzky and Golay 1964) obtained from ITT Visual Information Solutions' Code Contribution Library was applied to the spectra of the normalized images. The filter was adjusted to the fifth node left and right and a polynomial of third order.

Soil exclusion and spectral vegetation indices

Three approaches were tested for data extraction. In approach I, the complete image was defined as a region of interest (ROI) and spectral data were extracted from all pixels, plants and soil reflectance. For approach II, a mask for plant biomass was created by calculating the NDVI (Table 1) of the normalized image to exclude soil reflectance and to extract reflectance data of plant pixels only (NDVI > 0.5). The mask was applied to the normalized image and then reflectance was exported (Fig. 1a, b, c, d). For approach III, the margins of all leaves per plant were circumscribed manually by polygon-type ROIs; subsequently the mean spectrum of each plant within an image was extracted (Fig. 1e). In contrast to approach II, this leaf approach was used to obtain spectral information for the leaves of plants only, excluding petiole and soil reflectance.

For each ROI, the mean spectrum was calculated by ENVI and exported as ASCII file. This file was imported to MS Excel 2007 (Microsoft Corporation, Redmond, WA, USA) to calculate nine SVIs of spectra in a time series (Table 1). Spectral vegetation indices from remote sensing were tested for their correlation to ratings of above-ground disease symptoms depending on the method of image processing.

Table 1 Spectral vegetation indices used for correlation with leaf symptoms caused by *Rhizoctonia* crown and root rot

| Index	Equation	Reference
NDVI	$(R_{800} - R_{670})/(R_{800} + R_{670})$	Rouse et al. (1974)
Carter Index II	R_{695}/R_{760}	Carter et al. (1996)
Lichtenthaler Index I	$(R_{800} - R_{680})/(R_{800} + R_{680})$	Lichtenthaler et al. (1996)
OSAVI	$(1 + 0.16) \times (R_{800} - R_{670})/(R_{800} + R_{670} + 0.16)$	Rondeaux et al. (1996)
mCAI	$(R_{545} + R_{752})/2 \times (752–545) – \Sigma(R \times 2.8)$	Laudien (2005)
NDI	$(R_{750} - R_{705})/(R_{750} + R_{705})$	McNairn and Protz (1993)
SRPI	R_{430}/R_{680}	Penuelas et al. (1995)
PWI	R_{970}/R_{900}	Penuelas et al. (1997)
PRI	$(R_{550} - R_{531})/(R_{550} + R_{531})$	Gamon et al. (1992)
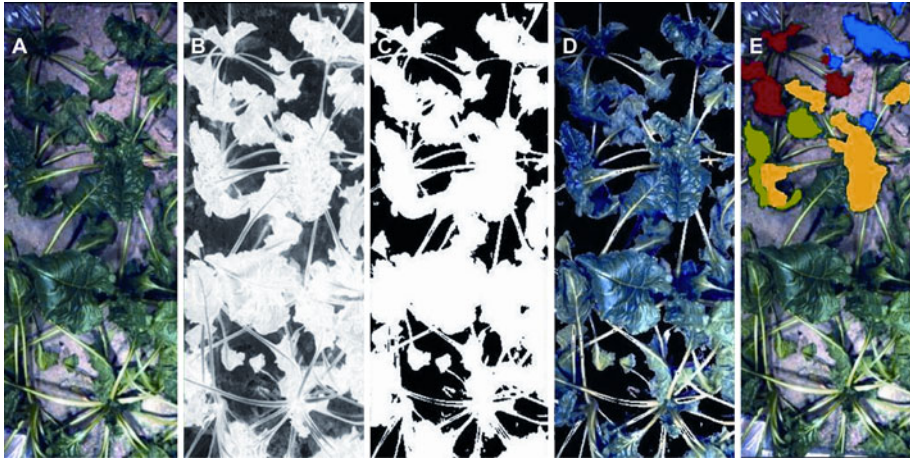
Fig. 1 Different stages of image processing: **a** normalized raw image, **b** NDVI transformed normalized raw image for creating a mask, **c** binary mask created from image (**b**), **d** mask applied to the normalized raw image (**a**), **e** regions of interest (ROIs) on leaves

Supervised classification

Hyperspectral images obtained by pre-processing approach II were used for supervised classification within the program ENVI (Fig. 1d). Four classes were formed; class 1: healthy; class 2: wilting; class 3: yellowing; class 4: tissue necrotic and brown. For each class, ROIs with 50 to 60 pixels were created in different images at locations with characteristic symptoms ($n = 5$). These classified ROIs were used to extract the pixels' mean spectra, which were saved as endmembers in a spectral library and used as references in the classification algorithm (Fig. 2).

The supervised classification method SAM was used, in which each pixel of the image was classified according to the endmember's spectra. For post-classification, a confusion matrix was applied to the classified image with five truth ROIs class^{-1} selected for

Fig. 2 Spectral library of signatures of sugar beet leaves with four classes of leaf damage/disease symptoms
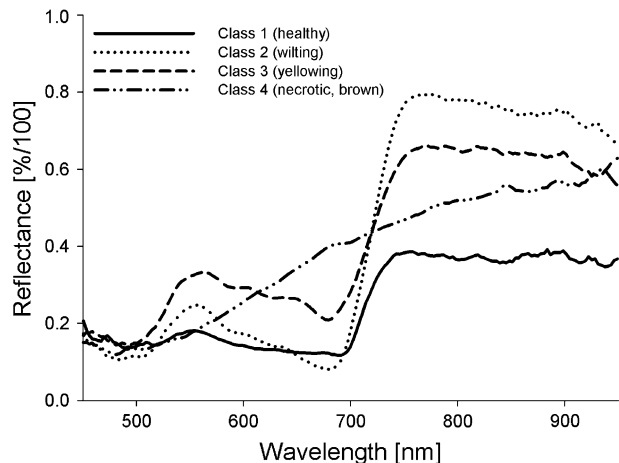
validation of the classification result. The confusion matrix results in an overall accuracy by summing the number of pixels classified correctly, divided by the total number of pixels. Additionally, the kappa coefficient (κ)—a statistical measure of inter-rater agreement for qualitative items—was calculated; it is a more robust measure than simple percent agreement calculation since κ takes into account the agreement occurring by chance (Cohen 1960).

Statistical analysis

The program PASW 18 (SPSS Inc., Chicago, IL, USA) was used for statistical analysis of data. Plant fresh weights were tested for homogeneity of variance and subsequently exposed to analysis of variance (ANOVA). Subgroups were built using Tukey's test with a probability level of $p < 0.01$. Plant weights were further analyzed by multi-factorial multi-variate analysis of variance (MANOVA) at a probability level of 0.01 with the factors *R. solani*, *H. schachtii* and *R. solani* × *H. schachtii*. MANOVA was used to test for statistical significance of the interaction between the organisms (Sikora and Carter 1987). Beet and leaf weights were tested for correlation at a probability level of 0.01 by Pearson's correlation coefficient. Correlations between plant weights, leaf symptom rating, RCRR beet rating and NDVI values were also calculated. Nine SVIs were correlated to leaf symptom ratings using Spearman's rank correlation coefficient. Leaf symptom ratings for RCRR were compared for each date using t test ($p < 0.05$). Also the *R. solani*-initiated beet surface rot rating and the number of eggs and J2 per plant were compared using the t test ($p < 0.05$).

Results

Visual development of plant-pathogen interactions

No differences were detected in plant development and leaf reflectance among treatments until 28 dai; neither *H. schachtii* nor *R. solani* produced visible above-ground symptoms. Leaf wilting became visible on BCN inoculated plants from 28 to 40 dai. Wilted leaves were detected predominantly for plants inoculated with *H. schachtii* alone. These observations were in accordance with the higher number of eggs and larvae in boxes inoculated with BCN alone compared to the combined inoculation (Table 2).

Forty days after inoculation, the first leaf symptoms caused by RCRR became visible at the petioles of the oldest leaves (Fig. 3). Leaf symptom ratings showed significant differences between the *R. solani* inoculated treatments starting 47 dai (Fig. 3). These symptoms, however, were not visible until 50 and 54 dai in the closed canopy of plants

Table 2 Influence of *Heterodera schachtii* and *Rhizoctonia solani* alone or in combination on the number of J2 larvae and eggs of *H. schachtii* per 100 g soil, and *R. solani* caused surface beet rot rating

Treatment	Number of eggs and J2	RCRR beet rating
Heterodera schachtii	12,375 ± 408 b	–
Rhizoctonia solani	–	2.97 ± 0.31 a
H. schachtii + *R. solani*	5,987 ± 257 a	5.13 ± 0.27 b

Columns with different letters indicate significant difference (t test, $p < 0.05$, $n = 32$)
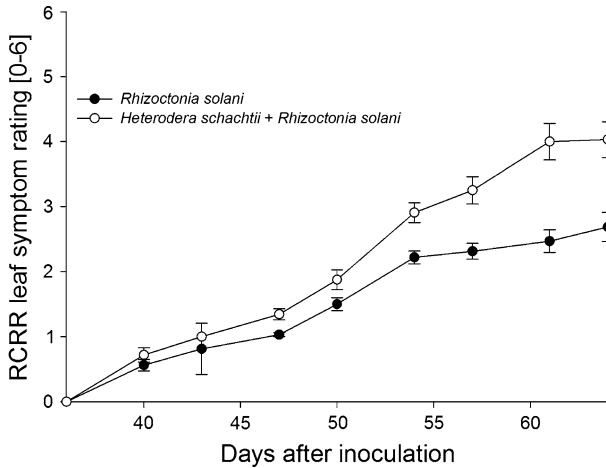
Fig. 3 Effect of *Rhizoctonia solani* alone and in combination with *Heterodera schachtii* on the development of sugar beet leaf symptoms. *Bars* indicate standard error of the mean (*n* = 32)

inoculated with the combination of *H. schachtii* and *R. solani* and with *R. solani* alone, respectively.

The number of eggs and larvae of *H. schachtii* was significantly higher in the treatment with the nematode alone compared to the mixed inoculation. Vice versa, beet rot was significantly more severe in the mixed inoculation compared to plants inoculated with *R. solani* alone (Table 2).

Leaf weights were closely correlated to beet weights ($r = 0.83$, $p < 0.01$). Leaves and beets of plants inoculated with the combination of *R. solani* and *H. schachtii* had the lowest biomass of all treatments (Fig. 4). According to the synergy factor (*SF*) modified after
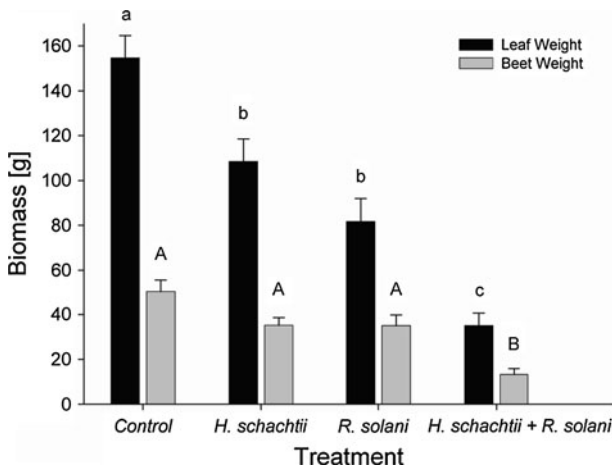

Fig. 4 Mean leaf and beet weight of sugar beet plants inoculated with either *Heterodera schachtii* or *Rhizoctonia solani* alone or with the combination of both pathogens. *Bars* represent standard error of mean. *Different letters* indicate significant difference among treatments according to Tukey's test ($p < 0.01$, *n* = 32)

Hillnhütter et al. ([2011b](#)), leaf weight was impacted in an additive way by disease complex ($SF = 1$), whereas beet weight resulted in synergistic damage ($SF = 1.2$). Multi-variate statistical analysis showed no interaction between BCN and RCCR for leaf and beet fresh weights, respectively ($F = 0.01$, d$f = 2$, $p = 0.98$ and $F = 0.68$, d$f = 2$, $p = 0.40$).

Effect of image processing on information from hyperspectral reflectance

Three different approaches to image processing were tested for their suitability to monitor symptom development caused by *H. schachtii*, *R. solani*, and the combination of both pathogens, respectively.

Biomass and plant vitality

The NDVI was calculated as a parameter for biomass/leaf area index and plant vitality for complete images including soil reflectance (approach I), images without soil reflectance (approach II), and images with leaf tissue only (approach III).

Calculations of the average NDVI from complete images overall resulted in slightly lower values than for the other image processing methods (Fig. 5). Leaf wilting of plants inoculated with *H. schachtii* resulted in lower NDVI values from 28 to 40 dai, for approach I (Fig. 5a). In contrast, methods excluding soil reflectance resulted in only marginal changes of NDVI. Forty dai, the BCN-inoculated plants recovered from wilting as demonstrated by NDVI values.

Starting 50 dai, the NDVI of sugar beet inoculated with both pathogens decreased; this effect was detected by all processing approaches (Fig. 5a, b, c). Using approach I, the NDVI of canopies of non-inoculated plants was higher than that of sugar beet inoculated with *R. solani* alone 64 dai and later (Fig. 5a). Image processing approach III—use of leaf pixels only—resulted in the discrimination between these treatments 7 days earlier (Fig. 5c). Approach II—exclusion of soil reflectance—was less sensitive in the discrimination of leaf symptoms caused by the pathogens (Fig. 5b).

The leaf weight of sugar beet plants was correlated to the NDVI calculated from approach one ($r = 0.61$, $p < 0.01$). As leaf symptom ratings were related to RCRR beet rot rating ($r = 0.93$, $p < 0.01$), the NDVI was also correlated to RCRR beet rot rating ($r = -0.84$, $p < 0.01$).

Spectral vegetation indices

Nine SVIs were tested for their suitability to discriminate between healthy plants and sugar beet with BCN infection and RCRR, respectively. The SVIs calculated from reflectance spectra considerably differed in their correlation to leaf symptoms depending on the image processing approach. Approach I, which included soil reflectance, resulted in the highest correlation between leaf symptom rating and NDVI (Table 3) by far. Approach II—exclusion of soil pixels—gave the highest correlations of pigment-specific SVIs to leaf symptom ratings. Especially indices related to photosynthesis—PRI, Lichtenthaler Index I, SRPI—gained the best correlations to visual symptom ratings ($r = -0.85$ to -0.88). In contrast, NDVI and PWI had the lowest correlation coefficients when using image processing approach II. The plant water index (PWI) was the only SVI which showed a significantly better correlation to leaf symptom ratings when applying image processing approach III (Table 3).
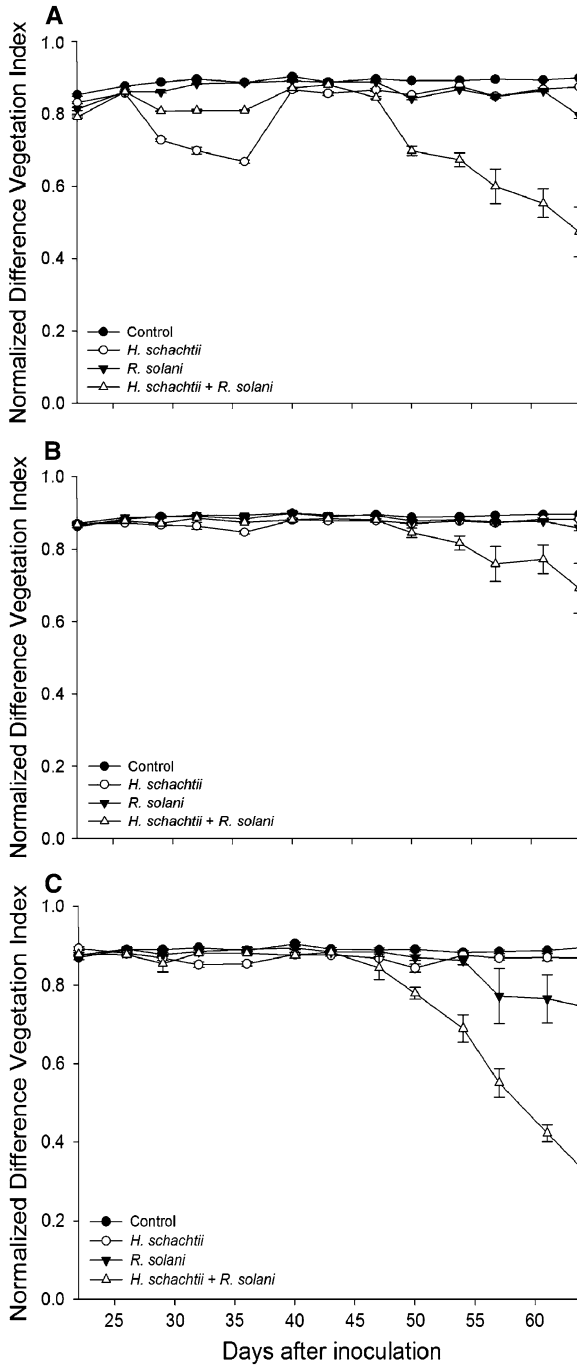
Fig. 5 Influence of image processing (**a** approach I [complete image], **b** approach II [soil reflectance excluded], **c** approach III [leaf reflectance only]) on NDVI calculated from spectra of sugar beet inoculated with either *Heterodera schachtii* or *Rhizoctonia solani* alone or with the combination of both pathogens. *Error bars* represent the standard error of the mean

Table 3 Spearman's correlation coefficient for the relation between leaf symptoms caused by *Rhizoctonia* crown and root rot and nine spectral vegetation indices depending on the pre-processing approach of hyperspectral images from sugar beet plants ($p < 0.01$, $n = 64$)

Index	Image processing approach		
	Complete image	Soil excluded	Leaves only
NDVI	−0.93	−0.69	−0.74
Carter Index II	0.73	0.71	0.73
Lichtenthaler Index I	−0.71	−0.86	−0.74
OSAVI	−0.73	−0.82	−0.69
mCAI	−0.71	−0.79	−0.65
NDI	−0.73	−0.80	−0.67
SRPI	−0.62	−0.85	−0.74
PWI	0.34	0.09	0.32
PRI	−0.71	−0.88	−0.78

Supervised classification

Based on four classes of increasing leaf damage severity, SAM classification was applied to images processed by approach II (Fig. 6). The confusion matrix of SAM results—comparison of classification to the four truth ROIs class^{-1}—indicated an overall accuracy of 79.4%. With a Kappa coefficient of $\kappa = 0.72$, a substantial agreement was achieved. There was some misclassification when comparing spectral library classification to truth ROIs. When comparing class 1 to 2, it resulted in 30% misclassification, because truth ROIs did not match with the spectral library classes (Table 4).
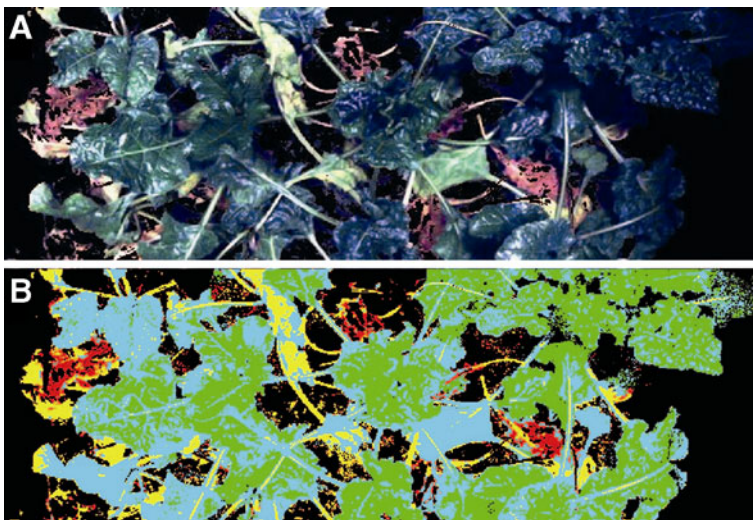

Fig. 6 Masked hyperspectral image **a** with different levels of damaged leaves and **b** the spectral angle mapper (SAM) classified image based on four classes (*green* class 1, healthy; *cyan* class 2, wilting; *yellow* class 3, yellowing; *red* class 4, necrotic and brown) from spectral library (Color figure online)

Table 4 Confusion matrix of four classes ImSpector image of spectral library endmembers with ground truth data

	Class	Ground truth				
		Class 1	Class 2	Class 3	Class 4	Total
Spectral library	Unclassified	0	0	10	1	3
	Class 1	71	0	0	0	22
	Class2	28	83	10	6	32
	Class 3	1	17	80	8	25
	Class 4	0	0	0	85	18
	Total	100	100	100	100	100

Agreement and disagreement of class-to-class comparison are given in percent

Discussion

Nematode-inoculated plants started to wilt after completion of the first generation cycle of *H. schachtii* due to the penetration of the second generation into the roots. The developmental stage of nematodes was calculated by the heat sum-model according to Čuri and Zmoray (1966) which confirmed time of initiation of first symptoms. After a heat sum of 465°C (32 dai), first wilting symptoms of leaves were detected. The plants recovered after about 10 days by the production of secondary roots which led to a reduction of leaf and beet masses (Cooke 1987).

Sugar beet inoculated with *H. schachtii* alone showed more severe wilting than plants inoculated with *R. solani* and *H. schachtii* together. The activity of *R. solani* is likely to inhibit the development of *H. schachtii* due to primary damage of the potential habitat of the obligate biotrophic nematode depending on vital root tissue. In contrast, development of RCRR was faster and more severe in the presence of BCN as compared to sugar beets attacked by *R. solani* alone. The fungal pathogen may be able to use the penetration sites of *H. schachtii* to enter the plants (Bergeson 1972). This leads to the conclusion that *H. schachtii* promotes the development of the fungal pathogen, whereas the fungus inhibits the development of the nematode. Synergistic effects between pathogens could not be proven statistically, in contrast to Hillnhütter et al. (2011b), which may be due to differences in experimental set-up. Nevertheless, the synergy factor showed a synergistic damage to the beet weight as reported by Hillnhütter et al. (2011b).

Significant correlations between biomass of leaves and beets demonstrated the close inter-relationship between leaves as the source of assimilates for beet development and the below-ground part for the uptake and allocation of water and nutrients. This balance between leaves and beets is the reason for the large potential of NDVI measurements for the assessment of below-ground damage of plants due to pathogens. Non-destructive hyperspectral sensing may be used in time series experiments on host-pathogen interactions as well as in screening systems for crop resistance to soil-borne pathogens and pests (Hillnhütter et al. 2010).

Three approaches to image processing were tested for their usefulness to assess the development of sugar beet symptoms due to the activities of *H. schachtii* and *R. solani*. The NDVI was confirmed to be a reliable indicator of ground cover and biomass of plants as reported by Rouse et al. (1974). Sensitivity was suitable to detect the wilting of leaves due to the penetration of second generation of *H. schachtii* larvae into roots, as well as the transient recovery of plants. Typically, symptoms of BCN include wilting due to drought

stress induced by root damage (Cooke 1987). Since leaves of wilted plants did not cover the soil as leaves of healthy plants did, increased soil reflectance decreased NDVI when approach I was used. This approach was similar to a non-imaging approach resulting in a spectral mixing of reflectance from crop and soil. In contrast, image processing approaches leading to pure plant reflectance resulted in only marginal changes of NDVI despite considerable leaf wilting. The NDVI *per se* is not suitable to assess the water status of plant tissue. Spectral vegetation indices sensitive to drought stress, therefore, should be tested for the detection of spectral differences between nematode-infested and unaffected plants.

Above-ground symptoms of RCRR include mainly yellowing of sugar beet leaves and the formation of a rosette of dying leaves on the soil in later stages (Herr 1996). Leaf symptoms were closely correlated to NDVI obtained from image approach I, whereas image processing approaches eliminating the soil gave considerably weaker correlations. The NDVI proved to be highly sensitive to changes in soil cover of crops. However, it seems not to be suitable for the detection of disease-specific modifications of plant tissue. Vice versa, pure plant pixel approaches are not very suitable for the assessment of crop biomass, unless the pixels classified as biomass are quantified.

The SVIs tested besides NDVI are mainly pigment specific (Lichtenthaler Index I, Carter II, mCAI, NDI, OSAVI, PRI, SRPI) or give information on the water status of plants (PWI). They are commonly used in remote sensing, but—similar to NDVI—largely lack specificity for the detection of plant diseases. Nevertheless, approach II with elimination of soil reflectance significantly increased their correlation to leaf symptom ratings. This approach has been described by Moshou et al. (2006) in order to remove soil reflectance for the discrimination of yellow rust from nutrient stress of wheat leaves. For RCRR-rating in sugar beet, the PRI had the highest correlation to leaf symptoms. It has been developed for tracking of photosynthetic light use efficiency (Gamon et al. 1992). The PRI proved to be more precise in the detection of physiological changes in leaves resulting from disease development than the NDVI as also stated by Gamon et al. (1992). Also the Lichtenthaler Index I, developed for the assessment of leaf fluorescence (Lichtenthaler et al. 1996) and the SRPI, related to carotenoids and chlorophyll a content of plant tissue (Penuelas et al. 1995), showed higher correlations to leaf symptoms.

The extraction of reflectance data by leaf-specific ROIs (approach III) gave the weakest correlations between SVIs and leaf symptoms incited by RCRR. This method was used by Rascher et al. (2007) for the assessment of leaf photosynthesis. The authors discussed its usefulness because of the manual selection of leaf area by ROIs and the non-normal distribution of data. Furthermore, manual selection is more time consuming than the use of a mask based on NDVI threshold values. Correlations between leaf symptoms and NDVI, Carter Index, and PWI were better in approach III than in the approach excluding soil only. This may be due to omitting the beet crown and petioles in ROIs. In addition, dead leaves selected by ROIs had spectral properties similar to the soil and contributed to the assessment of necrotic plant tissue as a leaf symptom of RCRR. A differentiation between BCN- and RCRR-affected sugar beet plants actually is only possible by taking into account the differences in the time of appearance of shoot symptoms.

Due to the lack of specificity of SVIs to characterize leaf symptoms of different diseases, a supervised classification method was tested. The SAM was useful to classify different disease states of leaves. A substantial inter-rater agreement shows the applicability of imaging sensor systems for disease symptom ratings. The spatial resolution of hyperspectral images in combination with the classification applicability is an enormous advantage to non-imaging sensors. Hyperspectral imaging in combination with SAM classification has been used successfully for quality management in fruits (Qin et al. 2009)

and could also be a useful tool for sugar beet breeders. Furthermore, the SAM method was used for the differentiation between above-ground symptoms of BCN and RCRR, respectively, and also for the quantification of RCRR severity from aerial field data (Hillnhütter et al. 2011a). The discrimination of symptoms and quantification of disease incidence reported by Hillnhütter et al. (2011a) can be used for site-specific management strategies in future studies.

Conclusions

Unprocessed images of sugar beet canopies allowed the assessment of differences in plant biomass as measured by NDVI. The elimination of pixels representing the soil or non-relevant plant tissue enabled the use of pigment-specific SVIs for the detection of physiological changes in plant tissue due to the development of root diseases. Therefore, leaf symptoms caused by either BCN or RCRR have to be investigated more in detail on the tissue level for characteristic differences in spectral reflectance. Disease-specific SVIs and/or combinations of existing SVIs may be applied in hyperspectral imaging of plant diseases in order to achieve an identification of diseases, improved quantification, and early detection of symptoms. The SAM classification seems to be a promising tool for the discrimination and quantification of diseases. This sensor technology in combination with leaf symptom classification can be effectively used by breeding companies for resistance tests. Furthermore, hyperspectral imaging can be used in field experiments to detect and discriminate stresses.

References

Ayoub, S. M. (1980). *Plant nematology—An agricultural training aid*. Sacramento: NemaÁid Publication.

Bajwa, S. G., Mishra, A. R., & Norman, R. J. (2010). Canopy reflectance response to plant nitrogen accumulation in rice. *Precision Agriculture, 11*, 488–506.

Bergeson, B. B. (1972). Concepts of nematode-fungus associations in plant disease complexes: A review. *Experimental Parasitology, 32*, 301–314.

Bravo, C. (2006). *Automatic foliar disease detection in winter wheat*. PhD Thesis, University Leuven, Belgium.

Carter, G. A., Dell, T. R., & Cibula, W. G. (1996). Spectral reflectance characteristics and digital imagery of a pine needle blight in the southern United States. *Canadian Journal of Forest Research, 26*, 402–407.

Clark, M. L., Roberts, D. A., & Clark, D. B. (2005). Hyperspectral discrimination of tropical rain forest tree species at leaf to crown scales. *Remote Sensing of Environment, 96*, 375–398.

Cohen, J. (1960). A coefficient of agreement for normal scales. *Educational and Psychological Measurement, 20*, 37–46.

Cooke, D. A. (1987). Beet cyst nematode (*Heterodera schachtii* Schmidt) and its control on sugar beet. *Agricultural Zoology Reviews, 2*, 135–183.

Čuri, J., & Zmoray, I. (1966). The relation of climatic factors to the duration of the development of *Heterodera schachtii* in Slovakia (ČSSR). *Helminthologica, 7*, 49–63.

Feilhauer, H., Oerke, E.-C., & Schmidtlein, S. (2010). Quantifying empirical relations between planted species mixtures and canopy reflectance with PROTEST. *Remote Sensing of Environment, 114*, 1513–1521.

Gamon, J. A., Penuelas, J., & Field, C. B. (1992). A narrow-waveband spectral index that tracks diurnal changes in photosynthetic efficiency. *International Journal of Remote Sensing, 41*, 35–44.

Heath, W. L., Haydock, P. P. J., Wilcox, A., & Evans, K. (2000). The potential use of spectral reflectance from the potato crop for remote sensing of infection by potato cyst nematodes. *Aspects of Applied Biology, 60*, 185–188.

Herr, L. J. (1996). Sugar beet diseases incited by *Rhizoctonia* species. In B. Sneh, S. Jabaji-Hare, S. Neate, & G. Dijst (Eds.), *Rhizoctonia species: Taxonomy, molecular biology, ecology, pathology and disease control* (pp. 341–349). Dordrecht: Kluwer Academic Publishers.

Hillnhütter, C., & Mahlein, A.-K. (2008). Early detection and localization of sugar beet diseases: New approaches. *Gesunde Pflanzen, 60*, 143–149.

Hillnhütter, C., Mahlein, A.-K., Sikora, R. A., & Oerke, E.-C. (2011a). Remote sensing to detect plant stress induced by *Heterodera schachtii* and *Rhizoctonia solani* in sugarbeet fields. *Field Crops Research, 122*, 70–77.

Hillnhütter, C., Schweizer, A., Kühnhold, V., & Sikora, R. A. (2010). Remote sensing for the detection of soil-borne plant parasitic nematodes and fungal pathogens. In E.-C. Oerke, R. Gerhards, G. Menz, & R. A. Sikora (Eds.), *Precision crop protection—The challenge and use of heterogeneity* (pp. 151–166). Dordrecht: Springer.

Hillnhütter, C., Sikora, R. A., & Oerke, E.-C. (2011b). Influence of different levels of resistance or tolerance in sugar beet cultivars on complex interactions between *Heterodera schachtii* and *Rhizoctonia solani*. *Nematology, 13*, 319–332.

Hooper, D. J., Hallmann, J., & Subbotin, S. (2005). Methods for extraction, processing and detection of plant and soil nematodes. In M. Luc, R. A. Sikora, & J. Bridge (Eds.), *Plant parasitic nematodes in subtropical and tropical agriculture* (pp. 53–86). Wallingford: CABI Publishing.

Kiewnick, S., Jacobsen, B. J., Braun-Kiewnick, A., Eckhoff, J. L. A., & Bergman, J. W. (2001). Integrated control of *Rhizoctonia* crown and root rot of sugar beet with fungicides and antagonistic bacteria. *Plant Disease, 85*, 718–722.

Kruse, F. A., Lefkoff, A. B., Boardman, J. W., Heidebrecht, K. B., Shapiro, A. T., Barloon, J. P., et al. (1993). The spectral image processing system (SIPS): Interactive visualization and analysis of imaging spectrometer data. *Remote Sensing of Environment, 44*, 145–163.

Kumar, L., Schmidt, K. S., Dury, S., & Skidmore, A. K. (2001). Imaging spectrometry and vegetation science. In F. van der Meer & S. M. de Jong (Eds.), *Imaging spectrometry* (pp. 111–155). Dordrecht: Kluwer Academic Publishers.

Laudien, R. (2005). *Entwicklung eines GIS-gestützten schlagbezogenen Führungsinformationssystems für die Zuckerwirtschaft. [Development of a field- and GIS-based management information system for the sugar beet industry].* PhD thesis, University of Hohenheim, Germany.

Lichtenthaler, H. K., Lang, M., Sowinska, M., Heisel, F., & Miehe, J. A. (1996). Detection of vegetation stress via a new high resolution fluorescence imaging system. *Journal of Plant Physiology, 148*, 599–612.

Mahlein, A.-K., Steiner, U., Dehne, H.-W., & Oerke, E.-C. (2010). Spectral signatures of sugar beet leaves for the detection and differentiation of diseases. *Precision Agriculture, 11*, 413–431.

McNairn, H., & Protz, R. (1993). Mapping corn residue cover on agricultural fields in Oxford county, Ontario, using thematic mapper. *Canadian Journal of Remote Sensing, 19*, 152–159.

Moshou, D., Bravo, C., Wahlen, S., West, J., McCartney, A., de Baerdemaeker, J., et al. (2006). Simultaneous identification of plant stresses and diseases in arable crops using proximal optical sensing and self-organizing maps. *Precision Agriculture, 7*, 149–164.

Mundt, J. T., Glenn, N. F., Weber, K. T., Prather, T. S., Lass, L. W., & Pettingill, J. (2005). Discrimination of hoary cress and determination of its detection limits via hyperspectral image processing and accuracy assessment techniques. *Remote Sensing of Environment, 96*, 509–517.

Noble, S.D., Crookshank, M. & Crowe, T.G. (2003). The design of a ground-based hyperspectral imaging/ imaging spectrophotometer system. Paper no.: 03-204. Resource document. Canadian Society of Bio-Engineering, Winnipeg, http://www.engr.usask.ca/societies/csae/PapersCSAE2003/CSAE03-204.pdf. Accessed 26 April 2011.

Nutter, F. W., Tylka, G. L., Guan, J., Moreira, A. J. D., Marett, C. C., Rosburg, T. R., et al. (2002). Use of remote sensing to detect soybean cyst nematode-induced plant stress. *Journal of Nematology, 34*, 222–231.

Oostenbrink, M. (1960). Estimating nematode populations by some selected methods. In J. N. Sasser & W. R. Jenkins (Eds.), *Nematology* (pp. 85–102). Chapel Hill: University of North Carolina Press.

Penuelas, J., Baret, F., & Filella, I. (1995). Semi-empirical indices to assess carotenoids/chlorophyll a ratio from leaf spectral reflectance. *Photosynthetica, 31*, 221–230.

Penuelas, J., Pinol, J., Ogaya, R., & Filella, I. (1997). Estimation of plant water concentration by the reflectance water index WI (R900/R970). *International Journal of Remote Sensing, 18*, 2869–2875.

Qin, J., Burks, T. F., Ritenour, M. A., & Bonn, W. G. (2009). Detection of citrus cancer using hyperspectral reflectance imaging with spectral information divergence. *Journal of Food Engineering, 93*, 183–191.

Rascher, U., Nichol, C. J., Small, C., & Hendricks, L. (2007). Monitoring spatio-temporal dynamics of photosynthesis with a portable hyperspectral imaging system. *Photogrammetric Engineering and Remote Sensing, 73*, 45–56.

Rondeaux, G., Steven, M., & Baret, F. (1996). Optimization of soil-adjusted vegetation indices. *International Journal of Remote Sensing, 55*, 95–107.

Rouse, J. W., Haas, R. H., Schell, J. A., & Deering, D. W. (1974). Monitoring vegetation systems in the Great Plains with ERTS. In *Proceedings of the third earth resources technology satellite-1 symposium* (pp. 301–317). Greenbelt: NASA.

Savitzky, A., & Golay, M. J. E. (1964). Smoothing and differentiation of data by simplified least squares procedures. *Analytical Chemistry, 36*, 1627–1639.

Schlang, J. (1991). Anbau resistenter Zwischenfrüchte zur biologischen Bekämpfung des Rübenzystennematoden. [Cultivation of resistant catch crops for biological control of the beet cyst nematode]. *Zuckerrübe, 40*, 476–488.

Schmitz, A., Tartachnyk, I. I., Kiewnick, S., Sikora, R. A., & Kühbauch, W. (2006). Detection of *Heterodera schachtii* infestation in sugar beet by means of laser-induced and pulse amplitude modulated chlorophyll fluorescence. *Nematology, 8*, 273–286.

Sikora, R. A., & Carter, W. W. (1987). Nematode interactions with fungal and bacterial plant pathogens - fact or fantasy. In J. A. Veech & D. W. Dickson (Eds.), *Vistas on nematology* (pp. 307–312). Hyattsville: Society of Nematologists.

Yang, C., & Everitt, J. H. (2002). Relationships between yield monitor data and airborne multidate digital imagery for grain sorghum. *Precision Agriculture, 3*, 373–388.

Yang, C., Everitt, J. H., & Bradford, J. M. (2008). Yield estimation from hyperspectral imagery using spectral angle mapper (SAM). *Transactions of the ASABE, 51*, 729–737.

Zens, I., Steiner, U. & Dehne, H.-W. (2002). Auftreten, Charakterisierung und Kontrolle des Erregers der Rübenfäule, *Rhizoctonia solani*, in Nordrhein-Westfalen. [Appearance, characterisation and control of the cause of *Rhizoctonia* crown and root rot, *Rhizoctonia solani*, in North Rhine-Westphalia]. *Landwirtschaftliche Fakultät der Universität Bonn, Schriftenreihe des Lehr- und Forschungsschwerpunktes USL, 91*, 1–105.